On Hysteresis at Axisymmetric Curved Shock Reflection from an Axial Cylinder

B. Shoesmith and E. Timofeev

Abstract The phenomena of hysteresis in the process of transition from regular to Mach reflection and back to regular reflection are studied using CFD to simulate the impingement of a curved axisymmetric incident shock on a cylinder placed along the axis of the flow. Pseudo-steady calculations conducted with decreasing and increasing cylinder radius are performed, causing a change in the incident shock strength that is sufficient to traverse the dual-solution domain in both directions. Hysteresis is shown to be present, although the points of transition are inconsistent with the detachment and von Neumann criteria.

1 Introduction

The process of transition from regular to Mach reflection (RR-MR) and back to regular reflection (MR-RR), in steady supersonic flow, is well known to exhibit hysteresis in certain cases [1]. Generally, to observe the RR-MR-RR hysteresis, it is necessary to traverse the dual-solution domain, where both RR and MR are physically admissible, in two opposite directions. This can be achieved by changing the wedge angle of the incident shock generator or by changing the freestream Mach number [1], which leads to changes in the shock angle. In axisymmetrical flows with a conical ring and a curvilinear cone, complex hysteresis phenomena were observed [1] for the situation when the conical converging shock generated by the ring was nearly straight, away from the centreline, with only minor variations of its angle.

It is known that converging axisymmetric shocks in steady supersonic flow steepen as they approach the centreline. The shock angle increases continuously from a point on the incident shock, leading to Mach reflection at the axis of symmetry [2]. When the shock impinges on an axial cylinder, the radius of the cylinder sets the incident shock angle, which leads to regular reflection at larger radii

B. Shoesmith (✉) · E. Timofeev
Department of Mechanical Engineering, McGill University, Montreal, QC, Canada
e-mail: ben.shoesmith@mail.mcgill.ca

A. Sasoh et al. (eds.), *31st International Symposium on Shock Waves 1*,
https://doi.org/10.1007/978-3-319-91020-8_105

and Mach reflection at smaller radii. This suggests that there is a range of centrebody radius where both types of shock reflections are possible, and therefore, it is possible to observe RR-MR hysteresis by changing the radius of the axial cylinder over time. The aim of this work is therefore to use a mesh-adaptive CFD code to apply this approach and to help understand the mechanisms responsible for transition to and from Mach reflection.

2 Approach

An axisymmetric wedge was used to generate the incident shock. This geometry generates a shock that strengthens continuously from the wedge surface as it approaches the axis. Downstream of the wedge, the surface is returned to the freestream direction, generating an expansion fan from the corner. This arrangement is shown in Fig. 1, where the incident shock is shown generating RR at larger cylinder radii and MR at smaller cylinder radii.

Method of characteristics (MOC) predictions were used to guide the choice of wedge angle. Calculations for a range of wedge angles were conducted to determine the incident shock geometry, and the approximate cylinder radii for shock detachment and reattachment were determined based on established criteria [1]. Figure 2 shows the cylinder radii at which the detachment and von Neumann conditions occur, plotted against initial shock angle at the wedge leading edge, for a freestream Mach number of 3.0. The shock angle is measured counter-clockwise from the axis of symmetry as shown in Fig. 1. As the initial shock strength increases, the minimum cylinder radius required during the simulation also increases, which reduces the size of the computational domain and of the associated mesh. Furthermore, the physical distance between the two limits also increases. This means that for a given minimum cell size, the region of shock between the two limits is more accurately resolved, which is advantageous when trying to locate points of transition. However, large changes in cylinder radius may require longer computation times and lead to a reduction in the quality of the mesh, which is stretched in order to compensate for the motion of the cylinder. A constraint on

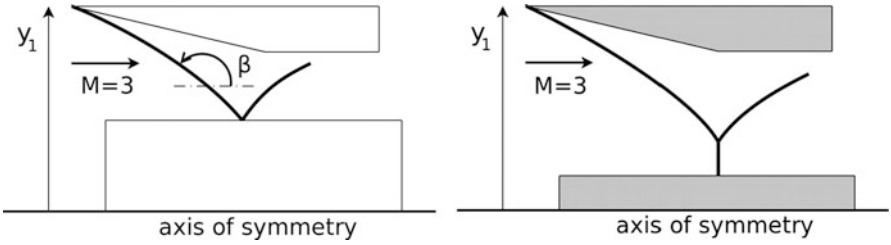

Fig. 1 Schematic showing regular and Mach reflection of a curved incident shock from cylinders of different radii

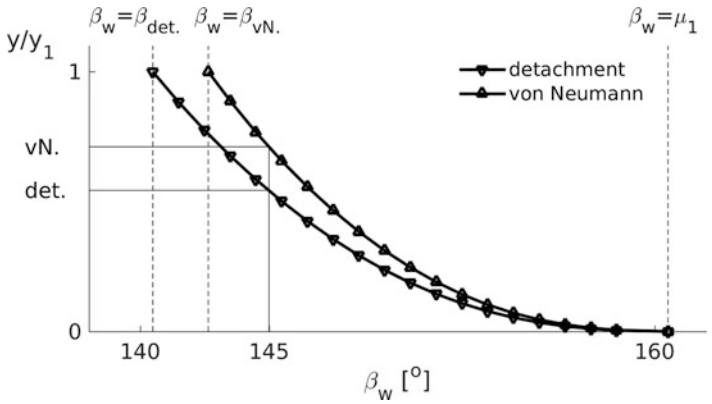

Fig. 2 Location of incident shock detachment and von Neumann limits as a function of shock angle at the wedge leading edge, β_w; μ is the Mach angle

Table 1 Location of shock reflection limits for a 145° initial shock angle at $M = 3.0$

	Shock angle, β	y/y_1
Detachment	140.480°	0.5420
Sonic	140.661°	0.5537
von Neumann	142.641°	0.7100

the chosen initial shock angle is that it must be greater than the von Neumann limit to allow for MR-RR as the cylinder radius increases. In practice, the initial shock angle must be somewhat greater than the von Neumann angle to allow transition to occur some distance away from the wedge surface. Based on this analysis, an initial shock angle of 145° was selected, which corresponds to a wedge angle of 17.58°. A corresponding summary of shock angles for shock detachment, sonic and von Neumann criteria, along with MOC predictions for the corresponding cylinder radii, is given in Table 1. A wedge length 0.5 (non-dimensionalised by wedge leading edge radius, y_1) was chosen based on guidance from MOC results. These results showed that the leading characteristic from the trailing edge expansion fan did not intersect the incident shock in the expected range of cylinder radii and, therefore, that the incident shock geometry was determined by the wedge geometry only. This choice of wedge length was also deemed to result in a moderate internal contraction ratio at the largest likely cylinder radius (at the von Neumann condition) and was therefore deemed unlikely to unstart the flow.

The numerical modelling results were obtained with an Euler (inviscid, non-heat-conducting) flow model. The gas (air) is assumed to be ideal with constant specific heats, with $\gamma = 1.4$. An adaptive unstructured finite-volume flow solver [3] is used. The solver employs a node-centred, second-order in space and time (for smooth solutions and uniform grids), MUSCL-Hancock TVD finite-volume scheme; see [4] for more details. A uniform background mesh is generated and used to begin the calculation. The mesh is then locally adapted to solution peculiarities (e.g. shock fronts, slipstreams, etc.) via an h-refinement procedure governed by a sensor based

on the normalized second derivative of density. Additional uniform refinement is applied in the regions deemed essential for computational accuracy.

The calculations presented here used a background mesh with a non-dimensional cell size of 0.02, although cells in the region containing the incident shock wave and the flow further downstream were given a minimum of three levels of refinement (cell size of $\sim 2.5 \times 10^{-3}$). The maximum number of refinement levels was typically set to 7 (cell size of $\sim 1.6 \times 10^{-4}$), with these cells typically used to resolve shocks. During the MR-RR calculation, the need to resolve extremely small Mach-stems close to the point of transition led to refinement levels as high as 11 (cell size of $\sim 9.8 \times 10^{-6}$), with a minimum level of 7 used in the region around the Mach-stem and in the flow immediately downstream.

As the cylinder is moved during the calculation, the background mesh is either stretched when the cylinder radius reduces or compressed when the cylinder radius increases, although the mesh is not regenerated during the calculation. This can lead to a reduction in cell quality when compared to the mesh prior to any movement of the cylinder. Therefore, in order to reduce the maximum amount of cell stretching at either extreme of the cylinder motion, the first calculation was conducted for a stationary cylinder with a radius of $y_{\mathrm{cyl}}/y_1 = 0.62$, which is mid-way between the detachment and von Neumann criteria values. This calculation was initialized with freestream conditions and produced a solution with RR at the cylinder surface. The cylinder radius was then reduced at a rate that gave the cylinder surface a Mach number of 0.05. The calculation was stopped regularly and ran to convergence with no cylinder motion, which helped to remove any uncertainty regarding the pseudo-steady nature of the cylinder motion. As a result, only these steady-state data points were used to assess the reflection type at that specific cylinder radius. The simulation was stopped when the flow transitions to MR, and a number of steady simulations were conducted in order to focus on the exact point of transition. In some cases that were known to be very close to transition, simulations were conducted with additional refinement in order to check for consistency. Taking a solution with Mach reflection to initialize the calculation, the cylinder radius was then increased with a Mach number of 0.05. Again, the simulation was stopped regularly and ran to convergence with the cylinder radius fixed. In this case additional regions of mesh refinement were added in order to resolve smaller Mach-stems and get closer to the point of transition, since it seemed that solutions with poorly resolved Mach-stems would revert to RR.

3 Results

Figure 3 shows results taken from the RR-MR and MR-RR calculations. RR-MR transition is predicted to occur between cylinder radii of $y/y_1 = 0.5228$ and $y/y_1 = 0.5226$. MOC predicted an incident shock angle of 140.1685° at $y/y1 = 0.5228$ and 140.1652° at $y/y1 = 0.5226$, a small change of only 0.0033°. However, both of these predictions correspond to noticeably smaller cylinder radii

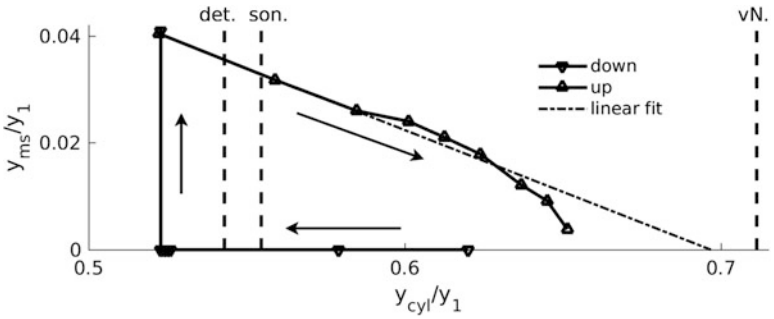

Fig. 3 Mach-stem height as a function of cylinder radius, for decreasing and increasing cylinder radius ('det', 'son' and 'vN' indicate the MOC-predicted radius for detachment, sonic and von Neumann limits, respectively)

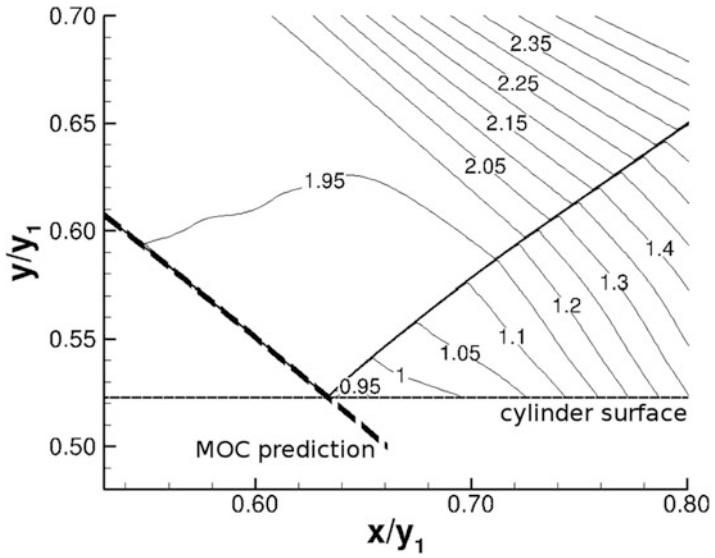

Fig. 4 RR at $y/y_1 = 0.5228$ (immediately before transition to MR)

than would be expected according to the detachment criterion (0.5420). Thus RR-MR transition is numerically predicted to occur at a shock angle ~0.31° steeper than the one corresponding to the detachment shock angle (140.480°). The reason for this discrepancy is currently unknown. The Mach number in the field immediately before transition to MR (Fig. 4) shows a small region of subsonic flow downstream of the point of shock reflection, which is consistent with the theoretical flow associated with the detachment criterion. It can also be seen that the reflected shock is curved, generating gradients in the downstream flow that cause it to accelerate in the streamwise direction. This acceleration is accompanied by a negative pressure gradient which would not typically contribute to the process of transition. These

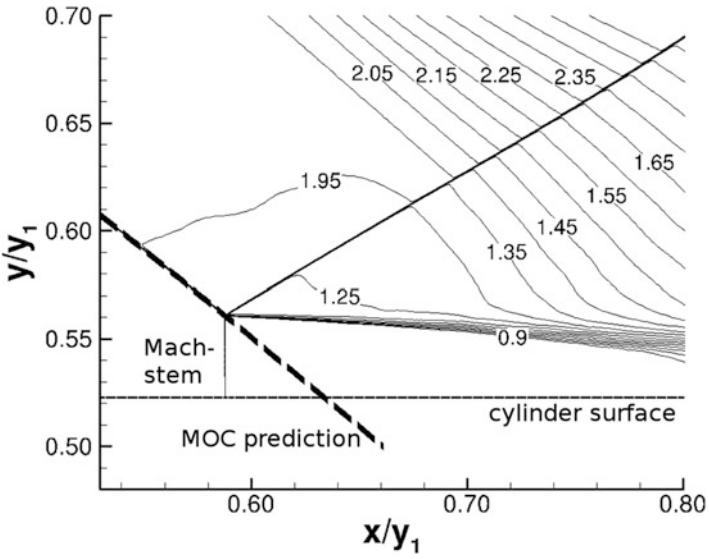

Fig. 5 MR at $y/y_1 = 0.5226$ (immediately after transition to MR)

observations are consistent with curved shock theory [5] and other results for regular shock reflection where the flow downstream of the reflected shock is fully supersonic [6]. The figure also shows the MOC-predicted incident shock location, and it is in very close agreement with the CFD.

Results for the calculation with an increasing cylinder radius show a gradual reduction in Mach-stem height. The relationship is not linear, with a more rapid reduction in Mach-stem height occurring towards the point of MR-RR transition. The trend, however, suggests that results for small Mach-stems are might be not fully mesh independent. A linear fit has however been applied to the data points for the three largest Mach-stems, and the estimated point of MR-RR transition is $y_{cyl}/y_1 = 0.6968$. This equates to a discrepancy of $\sim 0.14°$ in terms of shock angle when compared to the von Neumann criterion (0.7100). The Mach number in the field immediately after transition to MR is shown in Fig. 5. The triple point has effectively moved along the incident shock, producing a Mach-stem that is virtually straight and normal to the cylinder surface, generating relatively small stream-wise gradients in the downstream flow.

Flowfield results have revealed that the Mach-stream (flow between the cylinder surface and the shear layer) does not scale with the height of the Mach-stem. Instead, the distance from the Mach-stem to the sonic point (Mach-stream length), as a proportion of the Mach-stem height y_{ms}, increases significantly as the Mach-stem height reduces. For example, at the point of transition to MR, where $y_{ms}/y_1 = 0.04$, the ratio of Mach-stream length to Mach-stem height is 6.3. The equivalent value at $y_{ms}/y_1 = 0.004$ is 47. This makes it difficult to resolve the long shear layer and the Mach-stream close to MR-RR transition.

4 Conclusions

Pseudo-steady computations have been conducted in order to study the hysteresis associated with an axisymmetric shock impinging on a central cylinder. Results have confirmed the presence of hysteresis by demonstrating that RR and MR reflection can be obtained over a significant range of cylinder radii. Transition to MR occurs at a steeper incident shock angle than suggested by the detachment criterion (which seems to be consistent with other recent work, e.g. in [7]), and transition to RR occurs also at a steeper incident shock angle than would be suggested by the von Neumann criterion. The appearance of very high aspect ratio Mach-streams when the Mach-stem becomes small suggests that the predicted point of MR-RR transition may be particularly sensitive to the resolution of this feature.

Acknowledgement The present research is supported by the Fonds de recherche du Québec – Nature et technologies (FRQNT) and the National Science and Engineering Research Council (NSERC). B.S. gratefully acknowledges the McGill Engineering Doctoral Award (MEDA) funded in part by the Faculty of Engineering, McGill University. Rabi Tahir's support regarding the `Masterix` code is greatly appreciated.

References

1. G. Ben-Dor, *Shock Wave Reflection Phenomena*, 2nd edn. (Springer, Berlin, 2007)
2. A.I. Rylov, On the impossibility of regular reflection of a steady-state shock wave from the axis of symmetry. Appl. Math. Mech. **54**(2), 245–249 (1990)
3. Masterix, *ver. 3.40, RBT Consultants*, (Toronto, 2003–2015)
4. T. Saito, P. Voinovich, E. Timofeev, K. Takayama, Development and application of high-resolution adaptive numerical techniques in shock wave research center, In: *Godunov Methods: Theory and Applications*, ed. by E. F. Toro, (Kluwer Academic/Plenum Publishers, New York, 2001), pp. 763–784
5. S. Mölder, Curved shock theory. Shock Waves **26**(4), 337–353 (2015)
6. B. Shoesmith, S. Mölder, H. Ogawa, E. Timofeev, Shock reflection in axisymmetric internal flows, In: *Shock Wave Interactions, Selected Articles from the 22nd International Shock Interaction Symposium, University of Glasgow, UK, 4–8 July 2016*, ed. by K. Kontis, (Springer, Heidelberg, 2017), pp. 355–366
7. M.K. Hryniewicki, J.J. Gottlieb, C.P.T. Groth, Transition boundary between regular and Mach reflections for a moving shock interacting with a wedge in inviscid and polytropic air. Shock Waves Shock Waves **27**(4), 523–550 (2017)